EJMCiodidoPtII

DATASET · AUGUST 2015

READS
13

2 AUTHORS, INCLUDING:

Sinisa Radulovic
Institut za onkologiju i radiologiju Srbije
199 PUBLICATIONS **1,845** CITATIONS

SEE PROFILE

European Journal of Medicinal Chemistry 82 (2014) 372–384

Contents lists available at ScienceDirect

European Journal of Medicinal Chemistry

journal homepage: http://www.elsevier.com/locate/ejmech

Original article

Synthesis, characterization and cytotoxic activity of novel platinum(II) iodido complexes

Aleksandar Savić [a], Lana Filipović [b], Sandra Aranđelović [b], Biljana Dojčinović [c], Siniša Radulović [b], Tibor J. Sabo [a], Sanja Grgurić-Šipka [a, *]

[a] Faculty of Chemistry, University of Belgrade, Studentski trg 12-16, 11000 Belgrade, Serbia
[b] Institute for Oncology and Radiology of Serbia, Pasterova 14, 11000 Belgrade, Serbia
[c] Department of Chemistry, Institute of Chemistry, Technology and Metallurgy, University of Belgrade, Njegoševa 12, 11000 Belgrade, Serbia

ARTICLE INFO

Article history:
Received 17 February 2014
Received in revised form
28 March 2014
Accepted 25 May 2014
Available online 3 June 2014

Keywords:
Apoptosis
Cancer
Platinum complexes
Amine ligands

ABSTRACT

Novel Pt(II) complexes of general formula $[PtI_2(L^{1-3})]$, (**C1**–**C3**): where L^{1-3} are isobutyl, *n*-pentyl and isopentyl esters of (*S,S*)-1,3-propanediamine-*N,N'*-di-2-(3-cyclohexyl)propanoic acid has been synthesized and characterized by elemental analysis, UV/Vis, IR, (^{1}H, ^{13}C and HSQC, Pt) NMR spectroscopy and ESI mass spectrometry. Spectroscopic data and computational studies have shown the usual square planar coordination geometry of synthesized complexes, with coordination of ligands *via* nitrogen donor atoms. The cytotoxic activity of novel ligands and corresponding complexes were investigated on a palette of different cells line. Complexes **C1**–**C3** exhibited activity comparable to *cisplatin*, with IC_{50} values (μM) ranging from 4.6 ± 0.6 to 17.2 ± 2, and showed the highest potential in HeLa, LS-174 and EA.hy.926 cells. Ligands **L1**–**L3** exhibited two- to four-times less activity than corresponding complexes. Analysis of the mode of action in HeLa cells, by ICP-MS study, showed markedly higher intracellular accumulation and DNA binding affinity of **C1**–**C3** versus *cisplatin*, after 4 h and 20 h post-treatment. Annexin-V-FITC assay, flow cytometry and fluorescence microscopy study demonstrated occurrence of cell death through both apoptotic and necrotic changes. Tested complexes, at corresponding IC_{50} concentrations, caused considerable "sub-G1" peak, without other substantial alterations of cell cycle, while only **C1** induced higher level of phosphatidylserine externalization (11.7%), comparing to ligand **L1** (4.9%) and *cisplatin* (8.4%). Structure-activity comparison indicated variations of **C1**–**C3** cytotoxicity, related to the drug/ligand lipophilicity (C log P value), while intracellular platinum content and DNA platination increased on increase of length and branching of ester chain, in sequence: **C1** (isobutyl) < **C2** (*n*-pentyl) < **C3** (isopentyl).

1. Introduction

Metal complexes ensure a very diverse platform for drug design in the field of anticancer therapy. In addition to various oxidation states of metal ions, complexes of metals have different geometries and coordination numbers that allow the fine-tuning of their chemical reactivity [1–3]. In the last decades complexes with metal ions such as: platinum, ruthenium, gallium, gold, osmium and titanium have been investigated for their anticancer properties [4–6]. *Cisplatin* is still the most widely used metal-based drug in the treatment of different human tumors [7]. Among the second-generation platinum drugs, *carboplatin* and *oxaliplatin* has led to improvement in cancer therapy. Due to the many side effects of these drugs and cellular resistance, thousands of platinum complexes were synthesized, in order to find a more suitable antitumor drug [8,9]. The design of third generation platinum complexes was intended to overcome this problem. Diaminocyclohexane platinum complexes and their anticancer properties were intensively studied in recent years. *cis*-Dichlorido(1,2-aminocycloxexane)platinum(II) (DACHPt) is a *cisplatin* derivative with cyclohexane ring attached to the amino groups and this molecule has outstanding biological properties, much broader spectrum of activity and a lack of cross-resistance with *cisplatin* [10,11]. Unfortunately, this compound is completely insoluble in water and most other solvents, which is a problem in the application of this substance in biological systems. By substituting chlorides with oxalato ligand, in the mentioned compound, *oxaliplatin* was obtained and achieved worldwide clinical approval [12,13].

* Corresponding author.
E-mail addresses: sanjag@chem.bg.ac.rs, sanja.grguric@gmail.com (S. Grgurić-Šipka).

http://dx.doi.org/10.1016/j.ejmech.2014.05.060
0223-5234/

Platinum(II) compounds, of the type *cis*-$PtX_2(amine)_2$, where X is labile ligand (leaving anionic group) and an amine represents inert ligand (any primary or secondary amine or chelate amine ligand) exhibit significant anticancer activity against a variety of cell lines [14,15]. The most complexes of this type exhibit cytotoxicity by binding to DNA (in particular to the N7 atom of adjacent guanines), giving rise to a similar biological mode of action [16]. Also, platinum(II) complexes have shown reactivity toward different model proteins as well as to extra- and intracellular sulfur containing biomolecules [17–19]. Of the great interest as unconventional metal based drugs are the iodide analogs of *cisplatin*. These complexes were not interesting in medicinal chemistry because of their higher stability and lower reactivity of Pt–I bonds versus Pt–Cl bonds in aqueous solution [20]. A few papers can be found in the literature in which were described a special interactions of iodido platinum compounds with some important biomolecules. The significant difference in the reactivity of *cis/trans* iodido complexes was observed. In many cases it has been shown that the *trans* isomers may release their iodide ligands upon biomolecule binding, while the *cis* isomers preferentially release the amine ligands with retention of iodides [17,21,22]. Investigation of binding of these complexes to DNA models showed that both isomers bind with retention of amine ligand [17]. Pt(II) and Pt(IV) with ethylenediamine-*N,N′*-diacetate (edda)-type of ligand and their derivatives exhibit structure–activity relationships based on *in vitro* testing against of numerous cancer cell lines [23–25]. Esters of (*S,S*)-ethylenediamine-*N,N′*-di-2-(3-cyclohexyl)propanoic acid and corresponding platinum complexes showed enhanced biological activity in comparison to molecules with similar structure [26,27].

In an attempt to combine Pt(II) iododo complexes with derivatives of ethylenediamine-*N,N′*-diacetate (edda)-type of ligands, i.e., esters of (*S,S*)-1,3-propanediamine-*N,N′*-di-2-(3-cyclohexyl) propanoic acid to obtain new potent anticancer drugs, in this study we describe the synthesis, spectroscopic characterization, computational studies and *in vitro* biological evaluation of three new ligands and corresponding complexes. Promising biological activity and potential in *cisplatin* resistant cell lines provide useful information for further biological evaluation (interaction with small model proteins and oligonucleotides) and future drug design strategies.

2. Experimental

2.1. Chemistry

2.1.1. Starting agents

(*S*)-2-amino-3-cyclohexyl-propanoic acid hydrochloride was purchased from Senn Chemicals (Dielsdorf, Switzerland). (*S,S*)-1,3-propanediamine-*N,N′*-di-2-(3-cyclohexyl)propanoic acid dihydrochloride were prepared according to new procedure [28], while corresponding esters were obtained as described in this paper. $K_2[PtCl_4]$ was prepared by reduction of the $K_2[PtCl_6]$ with hydrazine [29]. Solvents were obtained commercially and used without further purification.

2.1.2. Measurements

Elemental analysis was carried out with Elemental Vario EL III microanalyzer. Infrared spectra were recorded on a Nicolet 6700 FT-IR spectrometer using the ATR technique. The NMR spectra (^1H, ^{13}C, HSQC and Pt) were recorded on a Bruker Avance III 500 spectrometer. Mass spectra of ligands were carried out with a 6210 Time-of-Flight LC-MS instrument (G1969A, Agilent Technologies) in methanol with addition formic acid. Mass spectra of complexes were carried out with an Orbitrap LTQ XL instrument (Thermo Scientific, Bremen, Germany) in 95% acetonitrile in water, with addition formic acid. Electronic spectra of 1×10^{-4} M solutions of platinum complexes were recorded in acetone, using a GBC UV/Vis Cintra 6 spectrophotometer. Melting points were determined on an Electrothermal melting point apparatus.

The lipophilicity parameters of the compounds were computed by employing the program available in the Internet (Alog PS 2.1-vcclab: C log P, Alog Ps, AC log P, milog P, KOWWIN, Xlog P2, Xlog P3 [30]). Prediction of lipophilicity by the Alog PS 2.1 program is described in two articles [31,32]. Clog *P* values were calculated by the ChemDraw Ultra 9.0 software [33].

2.1.3. Computational details

All calculations have been performed using the Amsterdam Density Functional (ADF) program package [34] version 2013.01, with general gradient approximation consisting of OPTX [35] for the exchange and PBE [36] functional for correlation (OPBE [37]). Molecular orbitals were expanded in an uncontracted set of Slater type orbitals (STOs) [38], of triple-ζ quality containing diffuse functions plus one set of polarization functions (TZP). Due to the presence of platinum, scalar relativistic corrections have been included self-consistently by using the zeroth-order regular approximation (ZORA) [39]. Default integration and gradient convergence criterions were used. Analytical harmonic frequencies [40] were calculated in order to ascertain that the optimized structures correspond to the minima on the potential energy surface. In order to check the possible influence of an environment, we also performed additional calculations with a dielectric continuum model (COSMO) [41] (using water as a solvent) as implemented in ADF [42].

2.2. Biology

2.2.1. Cell culture

Human cervical adenocarcinoma (HeLa), human alveolar basal adenocarcinoma (A549), human breast carcinoma (MDA-MB-231), human colorectal adenocarcinoma (LS-174), and human fetal lung fibroblast cell line (MRC-5), were maintained in the RPMI 1640 medium (Sigma Aldrich). The endothelial permanent human cell line derived by fusing human umbilical vein endothelial cells-HUVEC with human lung cells-A549 (EA.hy 926) was maintained in the nutrient medium, Dulbecco's Modified Eagle Medium (DMEM) (Sigma Aldrich). Both RPMI and DMEM media were supplemented with 10% heat inactivated fetal calf serum (FCS) (Sigma Aldrich), 4-(2-hydroxyethyl)piperazine-1-ethanesulfonic acid (HEPES) (25 mM), penicillin (100 units/mL), and streptomycin (100 mg/mL), while DMEM was additionally supplemented with D-Glucose (4.5 g/l). Cells were maintained as a monolayer culture in tissue culture flasks (Thermo Scientific Nunc™) in an incubator at 37 °C, in a humidified atmosphere composed of 5% CO_2.

2.2.2. MTT assay

Antiproliferative activity of tested complexes was determined using 3-(4,5-dymethylthiazol-yl)-2,5-diphenyltetrazolium bromide (MTT, Sigma–Aldrich) assay [43]. Cells were seeded into 96-well cell culture plates (Thermo Scientific Nunc™), at a cell density of 4000 c/w (HeLa), 8000 c/w (A549), 7000 c/w (LS-174, MDA-MD-231, MRC-5), 3000 c/w (EA.hy 926), in 100 μl of culture medium. After 24 h of growth, cells were exposed to the serial dilutions of the tested complexes. The complexes were dissolved in DMSO at a concentration of 10 mM as stock solution, immediately prior the use. Serial dilutions were made in culture medium so that final concentration of DMSO per well was less than 0.1% (v/v), in all experiments. Final concentrations achieved per wells were: 6.25 μM, 12.5 μM, 25 μM, 50 μM and 100 μM. Each concentration

was tested in triplicates. After incubation periods of 48 h, 20 μL of MTT solution, (5 mg/mL in phosphate buffer), pH 7.2 were added to each well. Samples were incubated for 4 h at 37 °C, with 5% CO_2 in humidified atmosphere. Formazan crystals were dissolved in 100 μL of 10% sodium dodecyl sulfate (SDS). Absorbances were recorded after 24 h, on an enzyme linked immunosorbent assay (ELISA) reader (Thermo Labsystems Multiskan EX 200–240 V), at the wavelength of 570 nm. IC_{50} values (μM), were determined from the cell survival diagrams. The percentages of surviving cells relative to untreated controls were determined. The IC_{50} value, defined as the concentrations of the compound causing 50% cell growth inhibition, was estimated from the dose–response curves.

2.2.3. Flow-cytometric analysis of cell cycle phase distribution

Quantitative analysis of cell cycle phase distribution was performed by flow-cytometric analysis of the DNA content in fixed HeLa cells, after staining with propidium iodide (PI) [44]. Cells were seeded at density of 2×10^5 cells/well at 6-well plate (Thermo Scientific Nunc™) and grown in nutrition medium. After 24 h cells were continually exposed to the investigated compounds or CDDP at concentrations corresponding to the 0.5× IC_{50} and IC_{50} values. After 24 h of continuous treatment cells were collected by trypsinization, washed twice with ice-cold PBS, and fixed for 30 min in 70% ethanol. After fixation cells were washed again with PBS, and incubated with RNaseA (1 mg/mL) for 30 min at 37 °C. Just before flow-cytometric analysis cells were stained with PI at concentration of 400 μg/mL. Cell cycle phase distribution was analyzed using a fluorescence activated sorting cells (FASC) Calibur Becton Dickinson flow cytometer and Cell Quest computer software.

2.2.4. Annexin V-FITC apoptotic assay

Quantitative analysis of apoptotic and necrotic cell death induced by the investigated platinum complexes and CDDP, as a referent compound, was performed by Annexin V-FITC apoptosis detection kit, according to the manufacturer's instructions (BD Biosciences). 2×10^5 HeLa cells were seeded into 6-well plates (Thermo Scientific Nunc™) in 2 mL of RPMI medium. After 24 h of growth, cells were treated with tested compounds or CDDP, for 6 h or 24 h, at concentrations corresponding to their IC_{50} values. Following treatment cells were washed twice with ice-cold PBS and then resuspended in 200 μl binding buffer (10 mM HEPES/NaOH pH 7.4, 140 mM NaCl, 2.5 mM $CaCl_2$). 100 μl of cell suspension (1×10^5 cells) was transferred to a 5 mL culture tube and mixed with 5 μl of Annexin V–FITC and 5 μl of propidium iodide (PI). Cells were vortexed and incubated for 15 min at 25 °C in the dark. After that, 400 μl of binding buffer was added to each tube and then analyzed using a FACS Calibur Becton Dickinson flow cytometer and Cell Quest computer software.

2.2.5. Measurement of intracellular platinum(II) accumulation using ICP-MS

Platinum accumulation was analyzed in HeLa cells, using inductively coupled plasma mass spectrometry (ICP-MS) using Thermo Scientific iCAP Qc ICP-MS (Thermo Scientific, Bremen, Germany) spectrometer with operational software Qtegra. HeLa cells were seeded into 75 cm^2 dish (Thermo Scientific Nunc™) and treated with the investigated complexes or CDDP at equimolar concentration of 10 μM. Following 4 h, cells were harvested by scraping, washed by ice cold PBS and cell pellet was collected by centrifugation at 2000 rpm, 10 min. Measurement of platinum(II) content in HeLa cells, was analyzed, using inductively coupled plasma mass spectrometry (ICP-MS) [45].

2.2.6. Measurement of platinum(II)-DNA-binding using ICP-MS

Binding of platinum to cellular DNA was analyzed in HeLa cells, using inductively coupled plasma optical emission spectrometry (ICP-MS) [45]. HeLa cells were seeded into 75 cm^2 dishes (Thermo Scientific Nunc™) and at the exponential phase of growth, cells were treated with the investigated complexes or CDDP at equimolar concentration of 10 μM. After 4 h treatment, cells were either collected, or medium was replaced by fresh medium and incubation continued for additional 20 h. Following treatment, cells were harvested by scraping, washed by ice cold PBS and cell pellet was collected by centrifugation at 2000 rpm, 10 min. Total DNA was isolated using TRI Reagent® (Sigma Aldrich) according to the manufacturer's procedure and concentrations were determined spectrophotometrically by measuring absorbance at A260/A280 nm (Eppendorf BioPhotometer 6131).

2.2.7. Fluorescent microscopy

HeLa cells (2×10^5 c/w) were seeded into 6-well plates (ThermoScientific Nunc™) in 2 mL of nutrient medium. After 24 h of growth, cells were exposed to the tested compounds or CDDP, at concentrations corresponding to their IC50 values. Following 6 h or 24 h of treatment, cells were stained with ethidium bromide (5 μg/mL) and acridine orange (1.5 μg/mL), and immediately after, observed under the fluorescent microscope Axio Observer Z1, using AxioVision imaging software (Carl Zeiss MicroImaging GmbH) [46].

2.2.8. Statistical analysis

Statistical analysis included testing of sample distribution for normality (Kolmogorov–Smirnov and Shapiro–Wilk tests; Q–Q Plot and Histogram), methods of descriptive statistics (mean, standard deviation [SD]), and testing the differences between the parameters (Kruskal–Wallis test, Wilcoxon rank sum and Wilcoxon signed rank tests). For multiple testing on the same cytotoxicity data set, the Bonferroni correction (0.05/15 = 0.0033) was used. Data analysis was performed using the statistical program R version 3.0.2.

2.3. Synthesis of ligands

*2.3.1. Synthesis of O,O′-diisobutyl-(S,S)-1,3-propanediamine-N,N′-di-2-(3-cyclohexyl)propanoate dihydrochloride, **L1***

Into the ice-cooled absolute isobutanol (30 mL), the thionyl chloride (4.5 mL) was added dropwise and then (*S,S*)-1,3-propanediamine-*N,N′*-di-2-(3-cyclohexyl)propanoic acid dihydrochloride (1.50 g, 3.30 mmol) was added. After stirring for 1 h, at 0 °C, suspension was refluxed for 24 h. Reaction mixture was filtered off and concentrated using water bath and after addition of acetone, left at 4 °C, over the night. The product was filtered, washed with absolute isobutanol and dried under *vacuo*. Compound **L1** is white powder. Yield: 0.82 g (42.5%); Mp: 208–210 °C; ^{1}H NMR (500.26 MHz, [D1]TFA): δ = 1.15 (d, (C***H*****3**)$_2$CHCH$_2$OOC–, 12H), 1.20 (m, C5a***H***, C5b***H***, 4H), 1.33–1.46 (m, C6a***H***, C6b***H***, 4H; C7***H***, 2H; N***H***, 1H), 1.69 (m, C4***H***, 2H), 1.86–2.01 (m, C5a***H′***, C5b***H′***, 4H; C6a***H′***, C6b***H′***, 4H; C7***H′***, 2H; N***H***, 1H), 2.09 (t, –C***H*****2**Cy, 4H), 2.19 (sept, (CH$_3$)$_2$C***H***CH$_2$OOC–, 2H), 2.81 (m, –NH$_2$CH$_2$C***H*****2**CH$_2$NH$_2$–, 2H), 3.60 and 3.71 (m, –NH$_2$C***H*****2**CH$_2$C***H*****2**NH$_2$–, 4H), 4.27 and 4.32 (m, (CH$_3$)$_2$CHC***H*****2**OOC–, 4H), 4.40 (t, –OOCC***H***–, 2H); ^{13}C NMR (125.79 MHz, [D1]TFA): 19.61 and 19.66 ((***C***H$_3$)$_2$CHCH$_2$OOC–) 25.86 (–NH$_2$CH$_2$***C***H$_2$CH$_2$NH$_2$–), 27.54 (***C7***), 27.67 and 27.69 (***C6a*** and ***C6b***), 29.76 ((CH$_3$)$_2$***C***HCH$_2$OOC–), 34.32 and 35.39 (***C5a*** and ***C5b***), 36.39 (***C4***), 39.86 (–***C***H$_2$Cy), 47.22 (–NH$_2$***C***H$_2$CH$_2$***C***H$_2$NH$_2$–), 62.42 (–OOC***C***H–), 77.19 ((CH$_3$)$_2$CH***C***H$_2$OOC–), 173.05 ppm (***C1***); IR (ATR): $\tilde{\nu}$ = 3434.8, 2927.1, 2853.9, 2714.7, 2652.9, 2371.8, 1746.2, 1540.1, 1469.6, 1373.3, 1277.3, 1199.6, 1068.6, 978.3 cm^{-1}; MS (LC-ESI): *m/z* 495.41 [M–2HCl + H]$^+$, 248.21 [M–2HCl + 2H]$^{2+}$; Anal. Calcd. for

$C_{29}H_{56}O_4N_2Cl_2 \cdot H_2O$, %: C 59.47, H 9.98, N 4.78. Found, %: C 59.23, H 9.58, N 4.81.

2.3.2. Synthesis of O,O′-dipentyl-(S,S)-1,3-propanediamine-N,N′-di-2-(3-cyclohexyl)propanoate dihydrochloride, L2

O,O′-dipentyl-(*S,S*)-1,3-propanediamine-*N,N′*-di-2-(3-cyclohexyl)propanoate dihydrochloride was prepared as described above using absolute *n*-pentanol. Compound **L2** is white powder. Yield: 0.79 g (39.1%); Mp: 182–184 °C; ^{1}H NMR (500.26 MHz, [D1] TFA): δ = 1.18 (t, C***H*****$_3$**$CH_2CH_2CH_2CH_2OOC$–, 6H), 1.25 (m, C5a***H***, C5b***H***, 4H), 1.43–1.56 (m, C6a***H***, C6b***H***, 4H; C7***H***, 2H; N***H***, 1H), 1.63 (m, CH_3C***H*****$_2$**$CH_2CH_2CH_2OOC$–, 4H; CH_3CH_2C***H*****$_2$**CH_2CH_2OOC–, 4H), 1.76 (m, C4***H***, 2H), 1.94–2.11 (m, C5a***H′***, C5b***H′***, 4H; C6a***H′***, C6b***H′***, 4H; C7***H′***, 2H; N***H***, 1H; $CH_3CH_2CH_2C$***H*****$_2$**CH_2OOC–, 4H), 2.17 (t, –C***H*****$_2$**Cy, 4H), 2.87 (m, $-NH_2CH_2C$***H*****$_2$**CH_2NH_2–, 2H), 3.69 and 3.78 (m, $-NH_2C$***H*****$_2$**CH_2C***H*****$_2$**NH_2–, 4H), 4.47 (t, –OOCC***H***–, 2H), 4.57 and 4.67 (m, $CH_3CH_2CH_2CH_2C$***H*****$_2$**OOC–, 4H); ^{13}C NMR (125.79 MHz, [D1]TFA): 14.59 (***C***$H_3CH_2CH_2CH_2CH_2OOC$–), 24.05 (CH_3***C***$H_2CH_2CH_2CH_2OOC$–), 25.86 ($-NH_2CH_2$***C***$H_2CH_2NH_2$–), 27.62 (***C7***), 27.74 (***C6a*** and ***C6b***), 29.97 (CH_3CH_2***C***$H_2CH_2CH_2CH_2OOC$–), 30.00 ($CH_3CH_2CH_2$***C***H_2CH_2OOC–), 34.34 and 35.45 (***C5a*** and ***C5b***), 36.46 (***C4***), 39.90 (–***C***H_2Cy), 47.26 ($-NH_2$***C***H_2CH_2***C***H_2NH_2–), 62.51 (–OOC***C***HNH_2–), 71.52 ($CH_3CH_2CH_2CH_2$***C***H_2OOC–), 173.07 ppm (***C1***); IR (ATR): $\tilde{\nu}$ = 2958.5, 2928.4, 2856.5, 2717.2, 2648.1, 2452.5, 2369.9, 1749.0, 1537.3, 1471.6, 1453.1, 1279.2, 1215.3, 1197.3, 1072.6, 1049.3, 968.3 cm^{-1}; MS (LC-ESI): *m/z* 523.44 $[M-2HCl + H]^+$, 262.22 $[M-2HCl + 2H]^{2+}$; Anal. Calcd. for $C_{31}H_{60}O_4N_2Cl_2 \cdot H_2O$, %: C 60.67, H 10.18, N 4.56. Found, %: C 60.76, H 9.71, N 4.61.

2.3.3. Synthesis of O,O′-diisopentyl-(S,S)-1,3-propanediamine-N,N′-di-2-(3-cyclohexyl)propanoate dihydrochloride, L3

O,O′-diisopentyl-(*S,S*)-1,3-propanediamine-*N,N′*-di-2-(3-cyclohexyl)propanoate dihydrochloride was prepared as described above using absolute isopentanol. Compound **L3** is white powder. Yield: 0.96 g (47.5%); Mp: 176–178 °C; ^{1}H NMR (500.26 MHz, [D1] TFA): δ = 1.10–1.20 (m, (C***H*****$_3$**$)_2CHCH_2CH_2OOC$–, 12H; $(CH_3)_2C$***H***CH_2CH_2OOC–, 2H; C5a***H***, C5b***H***, 4H), 1.33–1.44 (m, C6a***H***, C6b***H***, 4H; C7***H***, 2H; N***H***, 1H), 1.65 (m, C4***H***, 2H), 1.77–2.00 (m, C5a***H′***, C5b***H′***, 4H; C6a***H′***, C6b***H′***, 4H; C7***H′***, 2H; N***H***, 1H; $(CH_3)_2CHC$***H*****$_2$**CH_2OOC–, 4H), 2.01 (t, –C***H*****$_2$**Cy, 4H), 2.80 (m, $-NH_2CH_2C$***H*****$_2$**CH_2NH_2–, 2H), 3.60 and 3.70 (m, $-NH_2C$***H*****$_2$**CH_2C***H*****$_2$**NH_2–, 4H), 4.38 (t, –OOCC***H***–, 2H), 4.52 and 4.62 (m, $(CH_3)_2CHCH_2C$***H*****$_2$**OOC–, 4H); ^{13}C NMR (125.79 MHz, [D1]TFA): 11.80 and 17.06 ((***C***$H_3)_2CHCH_2CH_2OOC$–), 22.97 ($(CH_3)_2$***C***HCH_2CH_2OOC–), 25.79 ($-NH_2CH_2$***C***$H_2CH_2NH_2$–), 27.25 (***C7***), 27.65 and 27.73 (***C6a*** and ***C6b***), 34.27 and 35.36 (***C5a*** and ***C5b***), 36.33 (***C4***), 38.88 ($(CH_3)_2CH$***C***H_2CH_2OOC–), 39.79 (–***C***H_2Cy), 47.18 ($-NH_2$***C***H_2CH_2***C***H_2NH_2–), 62.42 (–OOC***C***HNH_2–), 69.91 ($(CH_3)_2CHCH_2$***C***H_2OOC–), 172.96 ppm (***C1***); IR (ATR): $\tilde{\nu}$ = 3468.0, 2929.3, 2855.8, 2719.2, 2653.3, 2448.8, 1744.0, 1539.4, 1471.7, 1367.0, 1338.0, 1277.4, 1237.6, 1199.8, 1139.1, 1069.8, 941.3 cm^{-1}; MS (LC-ESI): *m/z* 523.44 $[M-2HCl + H]^+$, 262.22 $[M-2HCl + 2H]^{2+}$; Anal. Calcd. for $C_{31}H_{60}O_4N_2Cl_2 \cdot 1.25H_2O$, %: C 60.22, H 10.19, N 4.53. Found: C 59.89, H 9.85, N 4.50.

2.4. Synthesis of complexes

2.4.1. Synthesis of [PtI$_2$(L1)], C1

To a solution of $K_2[PtCl_4]$ (50 mg, 0.12 mmol) in H_2O (1.5 mL) was added KI (99.6 mg, 0.6 mmol) and stirred for 5 min. Then a solution of ligand **L1** (70.28 mg, 0.12 mmol) in ethanol/water mixture (6 mL, 5:1), priorly neutralized with $LiOH \cdot H_2O$ (10.07 mg, 0.24 mmol) was added. The reaction mixture was stirred for 24 h, at room temperature in the dark. The precipitate was filtered off, washed with ethanol and dried in *vacuo*. Compound **C1** was isolated as a yellow powder. Yield: 78.34 mg (68.9%); Mp: 138–140 °C; ^{1}H NMR (500.26 MHz, [D1] $CDCl_3$): δ = 0.90–1.01 (m, dd, (C***H*****$_3$**$)_2CHCH_2OOC$–, 12H; C5a***H***, C5b***H***, 4H), 1.14–1.40 (m, C6a***H***, C6b***H***, 4H; C7***H***, 2H; $-NHCH_2C$***H*****$_2$**CH_2NH–, 2H; C4***H***, 1H), 1.52 (m, C4***H***, 1H), 1.68–1.94 (m, –C***H*****$_2$**Cy, 3H; C5a***H′***, C5b***H′***, 4H; C6a***H′***, C6b***H′***, 4H; C7***H′***, 2H), 2.03 (sept, $(CH_3)_2C$***H***CH_2OOC–, 2H), 2.48 (t, –C***H*****$_2$**Cy, 1H), 2.86 and 3.21 (m, $-NHC$***H*****$_2$**CH_2C***H*****$_2$**NH–, 4H), 3.89–4.06(m, $(CH_3)_2CHC$***H*****$_2$**OOC–, 4H), 4.76 and 4.88 (td, –OOCC***H***–, 2H), 5.61 and 6.02 (d, N***H***, 2H); ^{13}C NMR (125.79 MHz, [D1] $CDCl_3$): 19.26 and 19.30 ((***C***$H_3)_2CHCH_2OOC$–), 25.71 ($-NHCH_2$***C***H_2CH_2NH–), 26.00 and 26.26 (***C6a*** and ***C6b***), 26.41 (***C7***), 27.65 ($(CH_3)_2$***C***HCH_2OOC–), 32.38, 32.71, 33.13 and 34.32 (***C5a*** and ***C5b***), 33.83 and 35.28 (***C4***), 35.57 and 39.31 (–***C***H_2Cy), 50.41 and 51.28 ($-NHCH_2CH_2$***C***H_2NH–), 60.57 and 61.39 (–OOC***C***H–), 71.56 and 71.74 ($(CH_3)_2CH$***C***H_2OOC–), 170.72 and 171.22 ppm (***C1***); IR (ATR): $\tilde{\nu}$ = 3436.1, 3182.4, 3163.2, 2928.0, 2852.9, 1736.9, 1448.8, 1375.2, 1285.7, 1262.5, 1222.4, 1199.3, 1128.8, 1034.3, 1003.1, 960.7, 916.7 cm^{-1}; UV/Vis (acetone): λ_{max} (ε) = 376.86 nm (210 Lmol^{-1} cm^{-1}); MS: *m/z* 967.17 $[M + Na]^+$; Anal. Calcd. for $C_{29}H_{54}O_4N_2I_2Pt$, %: C 36.91, H 5.77, N 2.97. Found, %: C 36.76, H 5.66, N 3.18.

2.4.2. Synthesis of [PtI$_2$(L2)], C2

The complex **C2** was obtained as described for complex **C1** using 73.93 mg (0.12 mmol) of **L2**. The obtained compound is yellow powder. Yield: 71.42 mg (61.0%); Mp: 134–136 °C; ^{1}H NMR (500.26 MHz, [D1] $CDCl_3$): δ = 0.91–1.05 (m, C***H*****$_3$**$CH_2CH_2CH_2CH_2OOC$–, 6H), 1.10–1.29 (m, C5a***H***, C5b***H***, 4H; C6a***H***, C6b***H***, 4H; C7***H***, 2H), 1.32–1.45 (m, CH_3C***H*****$_2$**$CH_2CH_2CH_2OOC$–, 4H; CH_3CH_2C***H*****$_2$**CH_2CH_2OOC–, 4H); 1.46–1.76 (m, C5a***H′***, C5b***H′***, 4H; C6a***H′***, C6b***H′***, 4H; C7***H′***, 2H; $CH_3CH_2CH_2C$***H*****$_2$**CH_2OOC–, 4H; –C***H*****$_2$**Cy, 1H), 1.78–1.95 (m, C4, 2H; $-NHCH_2C$***H*****$_2$**CH_2NH–, 2H), 2.11 and 2.92 (m and t, –C***H*****$_2$**Cy, 3H), 2.73, 3.29 and 3.51 (m, $-NHC$***H*****$_2$**CH_2C***H*****$_2$**NH–, 4H), 3.61 and 3.77 (td, –OOCC***H***–, 2H), 4.22 and 4.36 (m, $CH_3CH_2CH_2CH_2C$***H*****$_2$**OOC–, 4H), 4.81 and 5.68 (d, N***H***, 2H); ^{13}C NMR (125.79 MHz, [D1] $CDCl_3$): 13.92 and 13.97 (***C***$H_3CH_2CH_2CH_2CH_2OOC$–), 19.77 ($-NHCH_2$***C***H_2CH_2NH–), 22.22 and 22.31 (CH_3***C***$H_2CH_2CH_2CH_2OOC$–), 25.67 and 26.05 (***C6a*** and ***C6b***), 26.14 and 26.29 (***C7***), 27.45 and 27.97 (CH_3CH_2***C***$H_2CH_2CH_2CH_2OOC$–), 28.12 and 28.16 ($CH_3CH_2CH_2$***C***H_2CH_2OOC–), 31.47 and 32.14 (***C5a*** and ***C5b***), 34.16 and 34.49 (***C4***), 35.18 and 37.24 (–***C***H_2Cy), 46.46 and 49.32 ($-NH$***C***H_2CH_2***C***H_2NH–), 61.96 and 62.46 (–OOC***C***HNH_2–), 66.33 and 66.50 ($CH_3CH_2CH_2CH_2$***C***H_2OOC–), 168.56, 170.53 and 173.40 ppm (***C1***); IR (ATR): $\tilde{\nu}$ = 3186.4, 3113.3, 2929.9, 2855.1, 1734.5, 1449.8, 1379.0, 1316.1, 1285.5, 1258.5, 1202.6, 1154.9, 1127.5, 1046.7, 993.5, 958.8, 917.5, 873.7, 735.2 cm^{-1}; UV/Vis (acetone): λ_{max} (ε) = 377.66 nm (136 Lmol^{-1} cm^{-1}); MS: *m/z* 972.22 $[M + H]^+$; Anal. Calcd. for $C_{31}H_{58}O_4N_2I_2Pt$, %: C 38.32, H 6.02, N 2.88. Found, %: C 38.00, H 5.84, N 2.88.

2.4.3. Synthesis of [PtI$_2$(L3)], C3

The complex **C3** was obtained as described for complexes **C1** using 74.47 mg (0.12 mmol) of **L3**. Compound **C3** is yellow powder. Yield: 74.33 mg (62.4%); Mp: 142–144 °C; ^{1}H NMR (500.26 MHz, [D1] $CDCl_3$): δ = 0.93–1.05 (m, (C***H*****$_3$**$)_2CHCH_2CH_2OOC$–, 12H), 1.10–1.40 (m. C5a***H***, C5b***H***, 4H; C6a***H***, C6b***H***, 4H; C7***H***, 2H; $(CH_3)_2C$***H***CH_2CH_2OOC–, 2H), 1.42–1.77 (m, C5a***H′***, C5b***H′***, 4H; C6a***H′***, C6b***H′***, 4H; C7***H′***, 2H; $(CH_3)_2CHC$***H*****$_2$**CH_2OOC–, 4H; –C***H*****$_2$**Cy, 1H), 1.78–2.10 (m, C***4***, 2H; $-NHCH_2C$***H*****$_2$**CH_2NH–, 2H), 2.10 and 2.89 (–C***H*****$_2$**Cy, 3H), 2.73, 3.31 and 3.52 (m, $-NHC$***H*****$_2$**CH_2C***H*****$_2$**NH–, 4H), 3.62 and 3.77 (m, td –OOCC***H***–, 2H), 4.00–4.40 (m, $(CH_3)_2CHCH_2C$***H*****$_2$**OOC–, 4H) 4.82 and 5.68 (d, N***H***, 2H); ^{13}C NMR (125.79 MHz, [D1] $CDCl_3$): 11.21 and 16.45 ((***C***$H_3)_2CHCH_2CH_2OOC$–), 19.71 ($-NHCH_2$***C***H_2CH_2NH–), 22.31 and 22.49 ($(CH_3)_2$***C***HCH_2CH_2OOC–), 24.98 and 25.63 (***C6a*** and ***C6b***),

26.06 and 27.05 (**C7**), 31.78 and 32.97 (**C5a** and **C5b**), 34.01 and 34.36 (**C4**), 35.18 and 37.11 (−**C**H_2Cy), 39.86 and 42.29 ($(CH_3)_2$CH**C**H_2CH_2OOC−), 46.53 and 49.43 (−NH**C**H_2 CH_2**C**H_2NH−), 61.96 and 62.52 (−OOC**C**HNH_2−), 64.55 and 64.87 ($(CH_3)_2CHCH_2$**C**H_2OOC−), 168.48, 170.51 and 173.40 ppm (**C1**); IR (ATR): $\tilde{\nu}$ = 3187.7, 3167.5, 2958.7, 2928.4, 2855.2, 1733.3, 1451.0, 1385.8, 1315.3, 1285.3, 1265.3, 1220.3, 1199.0, 1127.7, 1051.3, 993.5, 959.2, 919.8 cm^{-1}; UV/Vis (acetone): λ_{max} (ε) = 376.34 (132 $Lmol^{-1}$ cm^{-1}); MS: *m/z*, 972.22 $[M + H]^+$; Anal. Calcd. for $C_{31}H_{58}O_4N_2I_2Pt \cdot H_2O$, %: C 37.62, H 6.11, N 2.83. Found, %: C 37.20, H 5.78, N 2.85.

3. Results and discussion

3.1. Synthesis of ligands

Isobutyl, *n*-pentyl and isopentyl esters of (*S,S*)-1,3-propanediamine-*N,N′*-di-2-(3-cyclohexyl)propanoic acid dihydrochloride (**L1**−**L3**, Fig. 1A) have been obtained by the reaction of acid [28], corresponding absolute alcohol and thionyl chloride under reflux during 24 h. The obtained compounds are soluble in trifluoroacetic acid and formic acid.

3.2. Synthesis of complexes

Complexes of general formula, $[PtI_2(L^{1-3})]$ (**C1**−**C3**), (Fig. 1B) were prepared by the reaction of $K_2[PtCl_4]$ and the corresponding ligand in 1:1 M ratio, in the presence of excess KI. Reactions were performed in ethanol/water solution, at room temperature in dark for 24 h. The yellow complexes precipitated directly from the reaction mixture in moderate yields. Complexes are soluble in chloroform, acetone, dimethyl sulfoxide and partially soluble in ethanol.

3.3. Spectroscopic studies

Characteristic absorption band for C=O stretching vibration of ester was found in the IR spectra of the ligands (1746, 1749 and 1744 cm^{-1}) and complexes (1737, 1735 and 1733 cm^{-1}). These vibrations in the complexes were in the similar wave number as in the free ligands, indicating non-involvement of those groups into coordination. Also, C−O stretching vibrations for ligands and corresponding complexes were located in similar positions, in range 1199−1222 cm^{-1}. The IR spectra of complexes showed characteristic absorption bands for *val*(N−H) vibrations in the region of 3113−3188 cm^{-1}, indicating the coordination of esters ligands *via* nitrogen donor atoms. Typical *val*(C−N) vibrations appeared in the excepted region 1000−1300 cm^{-1}, for all synthesized compounds.

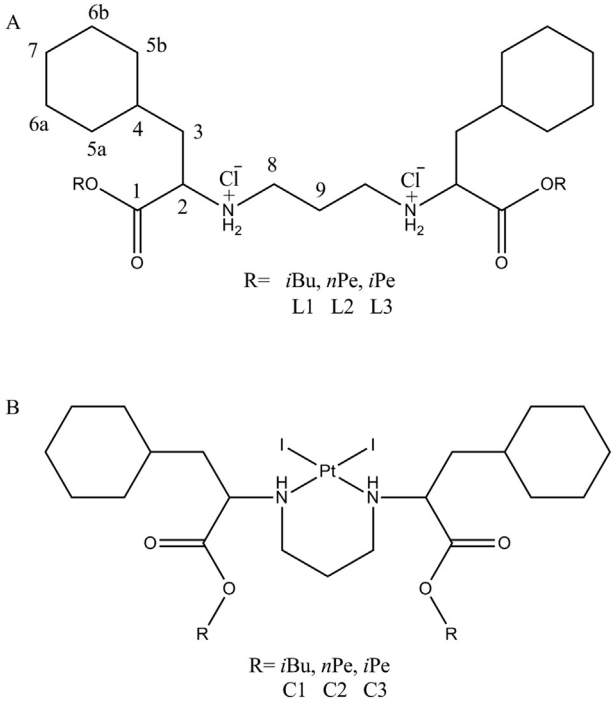

Fig. 1. Synthesized ligands **L1**−**L3** and complexes **C1**−**C3**.

In the ^{1}H NMR spectra of ligands and complexes, the signals attributable to cyclohexyl protons and alkyl groups from ester moiety (**R**CH_2O−) were in the range from 0.90 ppm to 2.11 ppm. The shift assignable to −NH_2**C**H_2**C**H_2**C**H_2NH_2− protons were shifted to higher field, while, N**H** protons were shifted lowerfield, after coordination. ^{1}H NMR spectra of complexes gave clear signals of R**C**H_2O− protons and these protons were detected in similar positions as in free ligands. In the ^{1}H NMR spectra of the ligands (recorded in TFA) protons of hydrochloride cannot be detected, because of the fast exchange these protons with solvent protons. In the ^{1}H NMR spectrum of ligand **L3**, which was recorded in DMSO, these protons were detected at 9.52 ppm. In the ^{13}C NMR spectra, all signals were detected at the expected chemical shifts. Cyclohexyl carbons in free ligands were found in the range of 27.25−36.46 ppm. In the ^{13}C NMR spectra of complexes these carbons were found in the region of 24.98−35.28 ppm. Carbons from diamine moiety in the free ligands were located around 25.80 ppm (−NH_2CH_2**C**$H_2CH_2NH_2$−) and 47.20 ppm (−NH_2**C**H_2CH_2**C**H_2NH_2−). Corresponding signals, in the ^{13}C NMR spectra of complexes, were found in region of 19.71−25.71 ppm (−NH_2CH_2**C**$H_2CH_2NH_2$−) and two signals between 46.46 and 51.28 ppm (−NH_2**C**H_2CH_2**C**H_2NH_2−). The carbon atoms of the R groups showed typical shifts for alkyl ester chain. Characteristic shifts for carbonyl group were detected at region of 168.48−173.40 ppm. In the ^{195}Pt NMR spectrum of complex **C1**, the chemical shifts appeared at − 3469 and − 3371 ppm. Two peaks on the close positions in ^{195}Pt NMR spectrum occur due to stereogenic nitrogen centers in the complex.

The mass spectra of the ligands contain peaks assigned to the $[M-2HCl + H]^+$ and $[M-2HCl + 2H]^+$ ions, which is in agreement with their calculated molecular mass. Molecular ions of complexes were detectable *m/z* at 967.17 $[M + Na]^+$ for **C1**, *m/z* at 972.22 $[M + H]^+$ for **C2** and **C3**. These values are in accordance with expected values.

3.4. Computational studies

DFT optimized global minimum energy structures of investigated complexes are given in Fig. 2. All three complexes showed square planar coordination around Pt^{2+} ion, with similar Pt−I (2.61−2.64 Å) and Pt−N (2.10−2.11 Å) bond lengths. The results follow the same trends irrespective of the environment (solvent or vacuum). Cartesian coordinates are given as Supplementary material.

3.5. Results of MTT assay

The antiproliferative activity of the ligands L: isobutyl (**L1**), *n*-pentyl (**L2**) and isopentyl (**L3**) esters of (*S,S*)-1,3-propanediamine-*N,N′*-di-2-(3-cyclohexyl)propanoic acid, and corresponding platinum(II) iodido complexes of structural formula $[PtI_2(L^{1-3})]$, (**C1**−**C3**), was evaluated for 48 h of continuous drug action, using colorimetric MTT assay. CDDP was used in this study, as a referent compound. Study was performed in five human neoplastic cell lines (HeLa, A549, MDA-MB-231, LS-174, EA.hy 926), and human fetal

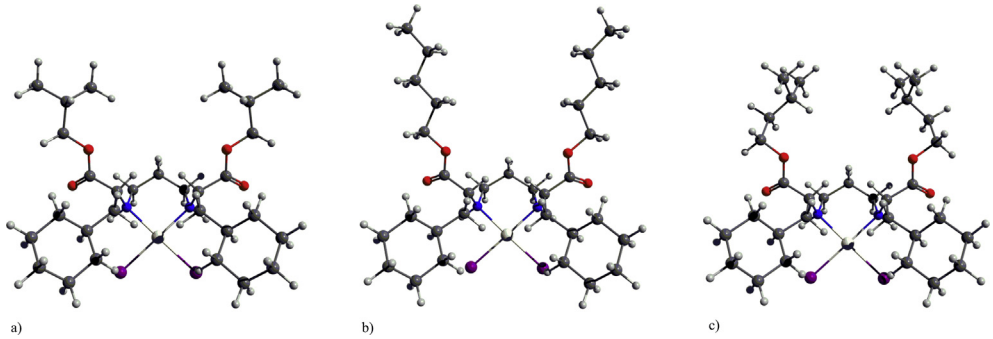

Fig. 2. DFT optimized global minimum energy of complexes: (a) **C1**; (b) **C2**; (c) **C3**.

lung fibroblast cell line (MRC-5), which was used as non-cancerous model for *in vitro* toxicity evaluation. Cytotoxicity of the complexes, summarized in terms of IC_{50} values, is presented in Table 1. The results showed that all compounds exhibited dose-dependent cytotoxicity in the range of concentrations up to 100 μM. Complexes **C1**–**C3** exhibited activity comparable to those of *cisplatin*, with the highest potential in HeLa, LS-174 and EA.hy 926 cells. HeLa cells were slightly more sensitive to the action of complexes **C2** and **C3**, than to the action of *cisplatin*, and obtained IC_{50} values (μM) were: 5.4 ± 1.2, 6.3 ± 1 and 6.9 ± 1.7, respectively. Notably, in LS-174 cells, the activity of **C1**–**C3** was about 3-fold, to 4-fold higher than that of *cisplatin*, and IC_{50} values (μM) decreased in sequence: 22.4 ± 0.4 (**CDDP**) < 8.6 ± 0.9 (**C1**) < 5.9 ± 1.1 (**C2**) < 5.5 ± 0.6 (**C3**). Ligands (**L1**–**L3**) showed approximately two- to four-times less activity comparing to the corresponding complexes, irrelevant to the target cell line. Ligands induced the highest cytotoxic effect in human transformed endothelial cells line (EA.hy 926), with IC_{50} values (μM) ranging from 9.1 ± 0.7 to 11.6 ± 0.8. EA.hy 926 cells were also the most sensitive to the action of **C1**, with IC_{50} (μM) 4.6 ± 0.6. Toxicity evaluation in MRC-5 cells, indicated slightly higher toxicity of **C2**, comparing to **CDDP**. MRC-5 and A549 cells were in general the least sensitive to the action of complexes and ligands. Statistical analysis of each cytotoxicity data for tested complexes and ligands (**C1**–**C3** and **L1**–**L3**) was done by Kruskal–Wallis test, and significant differences ($^*p < 0.05$), were observed for: **L3**, **C1** and **C3** (Table 1).

In vitro cytotoxic and anticancer potential of different esters of (*S,S*)-ethylenediamine-*N,N′*-di-2-(3-cyclohexyl)propanoic acid and the corresponding complexes with ruthenium and platinum(IV), have been already reported previously [26,27,47]. Esters of the (*S,S*)-ethylenediamine-*N,N′*-di-2-(4-methyl)pentanoic acid and their palladium complexes have also proven significant cytotoxic activity [48]. Structure-activity comparison in this study revealed that coordination of esters of (*S,S*)-1,3-propanediamine-*N,N′*-di-2-(3-cyclohexyl)propanoic acid to platinum(II) center, resulted in increased cytotoxicity of complexes, comparing to ligands. Cytotoxic activity of novel platinum(II)-iodido complexes of structural formula *cis*-[$PtI_2(L^{1-3})$] (**C1**–**C3**), was comparable or higher to those observed for *cisplatin*.

Efficient *in vitro* cytotoxicity of novel complexes may be explained by the influences of both leaving iodido ligands and carrier ligand (**L1**–**L3**) on complex reactivity. Previous structure-activity studies (Cleare et al.) of complexes of structure *cis*-[Pt(amine)$_2X_2$]; (X: Cl, I), indicated that chloride ion departs from Pt atom more quickly than the iodido ion, and that the ratio of the hydrolyzed platinum(II)(aqua)(hidroxo) species inside the cell and thus the kinetics of the reaction with cellular nucleophiles are different for chloride and iodide platinum analogues [49–51]. Six membered chelating ring formed by coordination to *N,N*-donors to platinum(II), in complexes **C1**–**C3**, certainly influenced steric environment around the metal center and kinetic of rupture of a Pt–I bond, in favor of better reactivity of **C1**–**C3** with target biomolecules [52–54]. Cytotoxic activity **C1**–**C3** was related to tumor cell species, but also differed with variation of esters groups in carrier ligands. With exception of MDA-MB-231 and EA.hy 926 cell lines, slight increase of cytotoxic activity of complexes was observed in relation to the increase of length or branching of the ester chain, in sequence: isobutyl < *n*-pentyl ≈ isopentyl. Previous studies of ruthenium or palladium complexes of similar structure, carrying chelating ligands such as *n*-alkyl esters of: (*S,S*)-ethylenediamine-*N,N′*-di-2-(3-cyclohexyl)propanoic acid or (*S,S*)-ethylenediamine-*N,N′*-di-2-(4-methyl)pentanoic acid, reported that increased lipophilicity of the ester groups (ethyl < *n*-propyl < *n*-butyl < *n*-pentyl) resulted in higher cytotoxic activity [27,47,48]. In order to determine whether, in the present study, IC_{50} values were in correlation to the corresponding lipophilicities of tested compounds, C log P values have been calculated, as a parameter of lipophilic efficiency, using ChemDraw Ultra 9.0 software (Table 2). Data obtained revealed that lipophilicity (C log P values) of ligands **L1**–**L3** increased in sequence: isobutyl (**L1**) < *n*-pentyl

Table 1
Table presents cytotoxicity of the tested agents and *cisplatin* in terms of IC_{50} values (μM), obtained for 48 h of continuous drug action, by MTT assay.

Compound	IC50 [μM] - (mean ± SD)						Kruskal–Wallis test	
	HeLa	A549	MRC-5	MDA-MB-231	LS-174	EA.hy 926	X^2_5	*p*-value
Complexes								
L1	13.7 ± 3.2	27.6 ± 5.1	30.6 ± 2.6	25.7 ± 0.3	27.6 ± 2.7	9.1 ± 0.7	9.791	0.081
L2	13.23 ± 2.7	31.1 ± 4.4	20.6 ± 9.4	31.3 ± 0.8	26.6 ± 2.9	11.6 ± 0.8	8.495	0.130
L3	16.4 ± 3.2	38.5 ± 1.7	26.2 ± 6.5	16.3 ± 1.5	27.5 ± 2.1	10.1 ± 1.3	11.847	*0.037
C1	7.2 ± 3.7	15.2 ± 2.3	17.2 ± 2.1	9.7 ± 0.5	8.6 ± 0.9	4.6 ± 0.6	11.475	*0.042
C2	5.4 ± 1.2	11.1 ± 3.6	11.9 ± 4.1	12.2 ± 0.4	5.9 ± 1.1	8.2 ± 0.2	8.483	*0.131
C3	6.3 ± 1.7	14.7 ± 4.2	14.2 ± 1.9	6.6 ± 0.5	5.5 ± 0.6	8.1 ± 0.8	11.608	0.040
Cisplatin	6.9 ± 1.7	17.2 ± 0.7	15.4 ± 3.1	21.9 ± 2.3	22.4 ± 0.4	27.7 ± 1.3	nd	nd

IC_{50} values present average (±SD) obtained from three or more independent experiments. $^*p < 0.05$, determined by statistical analysis of cytotoxicity data by Kruskal Wallis test. No additional significance was determined by further statistical analysis of the pair of groups: **L3**, **C1** and **C3**, using Wilcoxon rank sum test; nd: not-determined.

Table 2
Calculated lipophilicity parameters of the synthesized compounds.

Compound	Mr	C log P	A log Ps	AC log P	Milog P	kowwin	X log P2	X log P3
L1	496.76	9.337	2.03	5.63	4.41	7.13	6.96	8.49
L2	524.45	10.655	2.98	6.81	6.06	8.26	8.22	9.41
L3	524.45	10.395	2.42	6.56	5.48	8.12	8.10	9.20
C1	943.64	10.209	6.88	8.11	7.84	10.98	8.98	11.83
C2	971.69	11.527	7.57	8.35	8.35	11.13	9.11	12.04
C3	971.69	11.267	6.53	7.18	6.78	10.00	7.85	11.11

Cisplatin log P value = −2.53; Buβ et al.

(**L2**) ≈ isopentyl (**L3**), and that lipophilicity of the corresponding complexes **C1**–**C3** increased in the same order, depending of the alkyl-ester chain: **C1** (isobutyl) < **C2** (*n*-pentyl) ≈ **C3** (isopentyl). Apparently, minor variations in the length and branching of the alkyl-ester groups gave rise to the variations in lipophilic parameters and consequently in cytotoxic activity of tested platinum-iodido analogues.

3.6. Results of cell cycle analysis by flow cytometry

To determine whether the suppression of cancer cell growth by investigated agents was caused by a cell cycle arrest, HeLa cells were treated by investigated agents or *cisplatin* at IC_{50} or 0.5× IC_{50} concentrations, and cell cycle phase distribution was examined by flow cytometry, using staining with PI. At lower concentrations corresponding to 0.5× IC_{50}, complexes induced moderate changes of the cell cycle phase distribution (Fig. 3A.). **C1** induced slight and transient arrest in the S phase (26.5% comparing to control 21.3%), and G2-M phase (21.8% comparing to control 17.8%). **C3** also induced slight G2-M arrest (26.9%). At IC_{50} concentration **C1**–**C3** caused substantial loss of DNA from G2/M and late S-phase and generation of considerable "sub-G1" peak (Fig. 3B). Ligands **L1**–**L3**, did not significantly alter cell cycle progression. However *cisplatin* induced the concentration dependent population increase in the S phase (45.3% at 0.5× IC_{50} and 52.4% at IC_{50}). S phase arrest induced by *cisplatin* suggested block of DNA replication and was in agreement with the literature regarding effect of *cisplatin* on cell cycle progression [55,56]. Flow cytometry results suggested the occurrence of different mechanism of action of novel iodido–platinum complexes compared to *cisplatin*. Cytotoxic platinum(II) iodido complexes of a structural formula *cis*/*trans*-[PtI_2(amine)$_2I_2$], that exert their biological activity, without substantial effect on cell cycle progression, have been already described by Messori et al., [17]. However, **C1**–**C3** at IC_{50} concentration induced considerable accumulation of cells in sub-G1 fraction (Fig. 3B). Generation of "sub-G1" peak is considered as a hallmark of internucleosomal DNA cleavage catalyzed by nucleases in the course of apoptotic cell death [57], though there are evidences that DNA cleavage might occur independently from executor caspases [58,59]. Cytotoxic agents may induce DNA breaks in direct interaction with DNA, particularly at high levels of damage, which is more likely to be mechanism of action of iodido platinum(II)-based complexes [17,58].

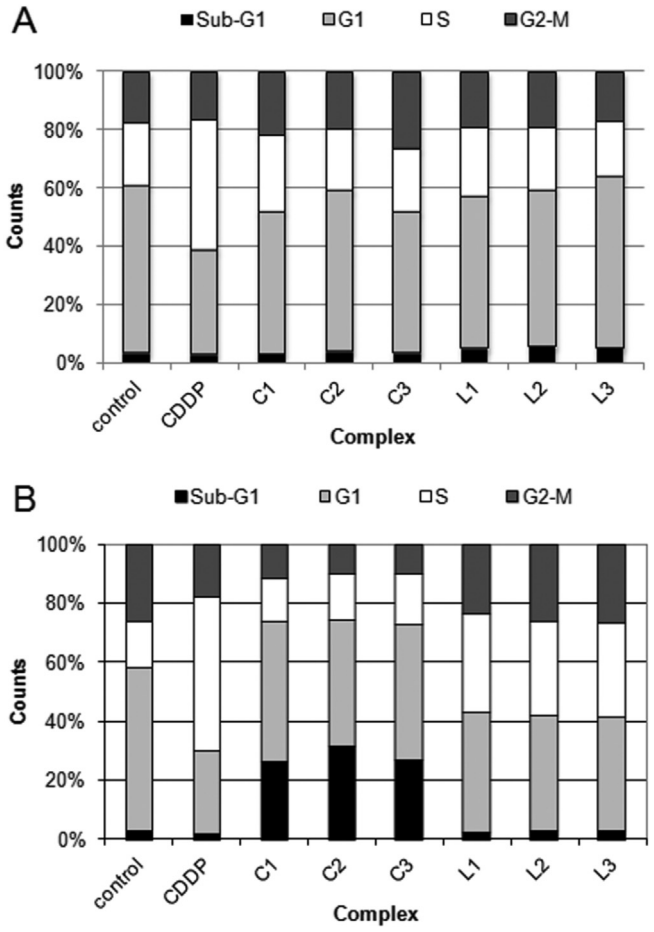

Fig. 3. Diagrams presenting cell cycle phase distribution of treated HeLa cells, obtained by flow-cytometric analysis of the DNA content in fixed cells, after staining with PI. HeLa cells were collected following 24 h treatment with tested complexes or **CDDP** at concentration corresponding to (A) 0.5 × IC_{50} and (B) IC_{50}. Bar graphs represent mean ± SD in at least three independent experiments.

3.7. Results of Annexin-V-FITC apoptosis assay

Potential of the investigated compounds or *cisplatin* to induce apoptosis in HeLa cells was analyzed following 6 h or 24 h of treatment with IC_{50} concentrations, by flow cytometry, following Annexin-V-FITC/propidium iodide dual staining. As phosphatidylserine (PS) exposure usually precedes loss of plasma membrane integrity in apoptosis, the presence of Annexin-V-FITC labeled cells is considered as indicator of apoptosis [59]. Data obtained are presented in Figure (Fig. 4B), as a percentages of an early apoptotic cells, FITC(+)PI(−); late apoptotic cells, FITC(+)/PI(+); and necrotic cells, FITC(−)/PI(+). Representative dot plot diagrams obtained for 6 h of drug action, are presented in (Fig. 4A). Results indicated that **C1** and **C3**, as well as the ligands **L1**–**L3**, induced apoptotic changes following short-term (6 h) treatment. **C1** initiated apoptosis, in terms of FITC(+)PI(−) staining, to a larger extent (11.7%) than ligand **L1** (4.9%) and *cisplatin* (8.4%). **C2** as well as **L2** exhibited the least potential for apoptosis induction. Both ligands and complexes induced significant percentage of cells stained by FITC(+)/PI(+) or FITC(−)/PI(+), following 6 h or 24 h treatment. How cell death proceeded to later stages, rupture of a cell membrane allowed secondary apoptotic and necrotic cells to stain intensely with both probes [59]. Data obtained suggested that investigated compounds induced cell death at least partly (initially), by apoptosis. However, **C2** and **C3** exhibited reduced potential for apoptosis induction in comparison to ligands **L2** and **L3**. Knowledge of the relationship between the ligand structure and the cytotoxicity of the Pt-based complexes is still limited. According to the results obtained, mode of action of complexes could not be simply predicted upon structure or mode of cytotoxic action of ligands. It is known that the chemistry of platinum complexes is dominated by the affinity of Pt(II) center toward amine ligands and nucleophilic targets in the cell, such as DNA [50,55]. Nevertheless, recent study suggested that

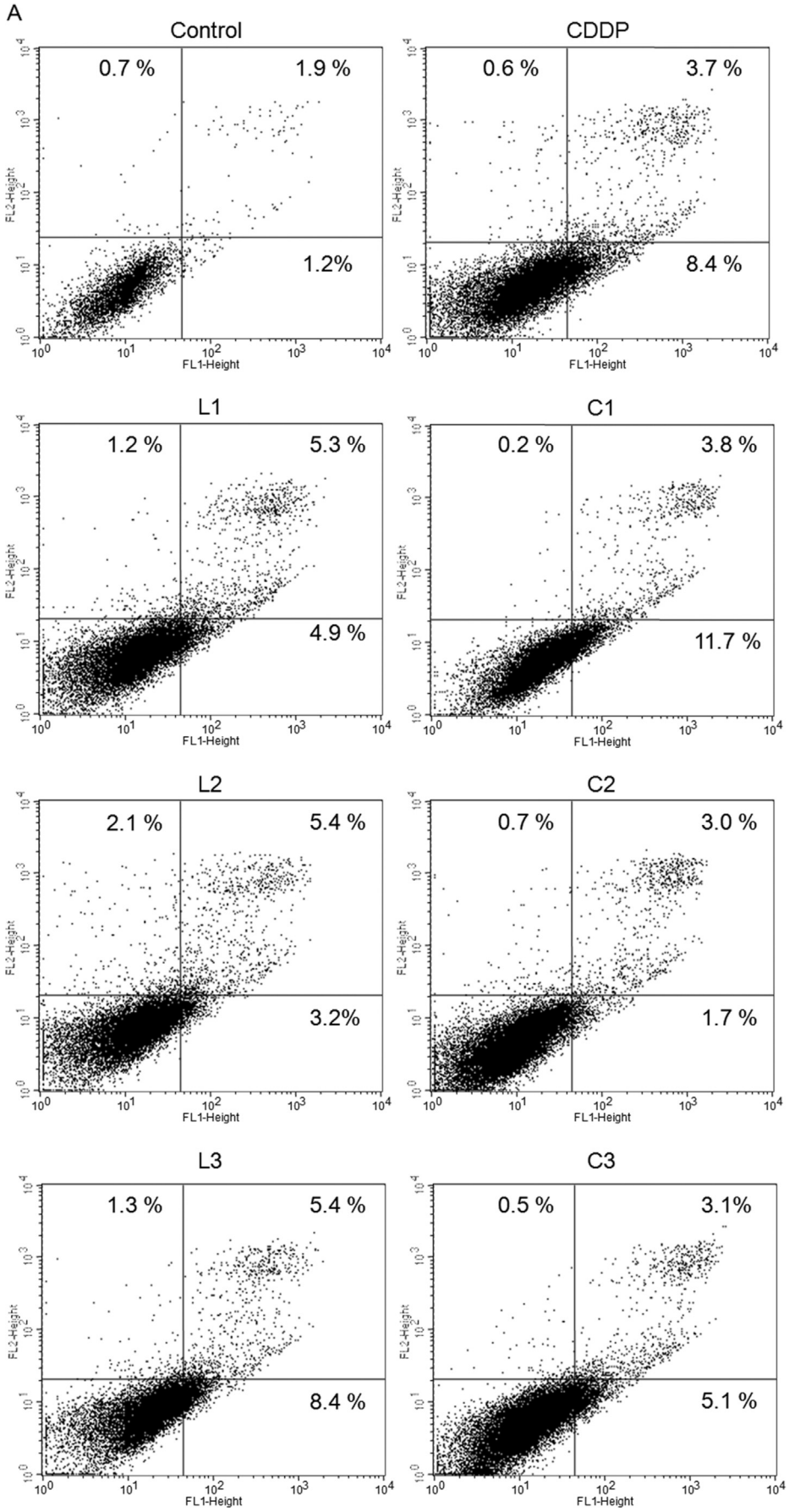
A
Control
0.7 %
1.9 %
1.2%
CDDP
0.6 %
3.7 %
8.4 %
L1
1.2 %
5.3 %
4.9 %
C1
0.2 %
3.8 %
11.7 %
L2
2.1 %
5.4 %
3.2%
C2
0.7 %
3.0 %
1.7 %
L3
1.3 %
5.4 %
8.4 %
C3
0.5 %
3.1%
5.1 %
FL1-Height
FL2-Height

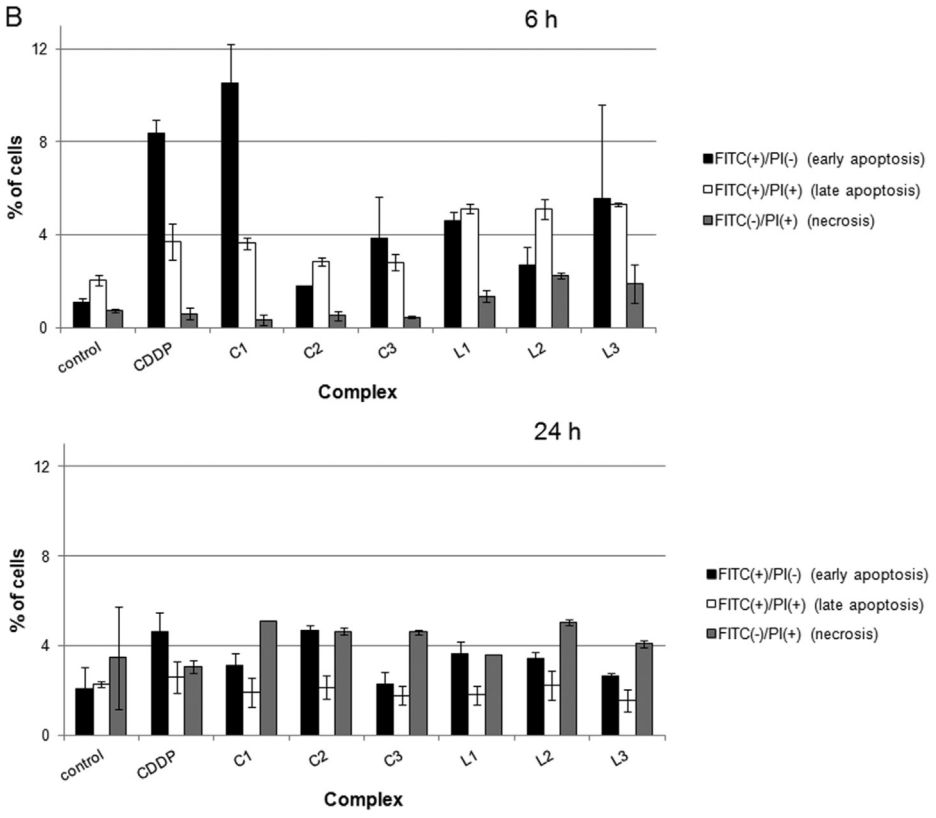

Fig. 4. (*continued*).

diiodido-diamine Pt(II) complexes, apart from the preferential binding to nuclear DNA, exhibited different pattern of interaction to cellular proteins, comparing to *cisplatin* [17]. Alternatively, some extra-nuclear damages such as inhibition of catalytic activity of apoptotic-executor caspases or depletion of ATP production, may result in an impairment of initial apoptotic process and block progression of cell death to a typical apoptotic phenotype [59]. Precise mechanism of cell death induction by tested complexes and factors that lead to the onset of apoptotic/necrotic changes, still remain to be investigated.

3.8. Results of ICP-MS measurement of intracellular platinum(II) accumulation

In order to investigate level of intracellular platinum(II) accumulation of novel iodido-platinum(II) complexes comparing to *cisplatin*, intracellular platinum content was analyzed in HeLa cells treated with equitoxic concentrations of the investigated complexes, or *cisplatin* (10 μM), for 4 h using ICP-MS. The level of Pt found in cells after the treatment, was normalized upon the cell number in order to obtain the intracellular Pt concentration (μgPt/10^6 cells), and results are presented in Fig. 5A. Data obtained indicated that tested complexes entered cells markedly more efficiently comparing to *cisplatin* and intracellular platinum concentration (μgPt/10^6 cells), increased in sequence: **CDDP** (2.5 ± 0.01) < **C1** (10.1 ± 0.1) < **C2** (11.6 ± 0.1) < **C3** (14.5 ± 0.1). Comparison with the results of MTT study revealed correlation to the cytotoxicity of complexes **C1**–**C3**, which was in accordance to the literature considering biologically active platinum compounds. Number of studies highlighted the relevance of the influx of platinum complexes for the activity, as there is a clear relationship between DNA platination and cytotoxicity of *cisplatin* in numerous cell line pairs [61–64]. The significant increase of intracellular platinum accumulation of **C1**–**C3** ($^*p < 0.05$; Kruskal Wallis test), comparing to *cisplatin* (Fig. 5A), seemed to be due to the structural characteristics of the non leaving ligands, carrying ester groups. Structure activity comparison in this study, indicated that intracellular accumulation of tested complexes increased in relation to the length and branching of ester groups, in sequence: isobutyl (**C1**) < *n*-pentyl (**C2**) < isopentyl (**C3**). Since platinum drug accumulation may depend on drug lipophilicity, as suggested by several studies, we calculated C Log P value (parameter of lipophilicity), for **C1**–**C3** and **L1**–**L3**, as an indicator of compound ability to pass through the cell membrane [19,23,24]. Theoretically calculated values C Log P for complexes, increased in sequence: 10.2 (**C1**) < 11.3 (**C3**) ≈ 11.5 (**C2**), (Table 2.), and were shown in fact, to be similar in complexes with pentyl-esters groups: **C2** (*n*-pentyl) and **C3** (isopentyl). Lipophilicity of cisplatin (log P value = −2.53; Buβ [65]) was available from literature data [65]. There was correlation of **C1**–**C3** lipophilicity to the significantly enhanced accumulation of **C1**–**C3** ($^*p < 0.05$) versus *cisplatin*. Moreover, the highest intracellular platinum content of **C3**, even superior to **C2** (Fig. 5A),

Fig. 4. (A) Dot plot diagrams obtained by flow-cytometric analysis of treated HeLa cells after dual staining with Annexin-V-FITC and PI. Annexin-V-FITC/PI staining was monitored in HeLa cells, following 6 h or 24 h treatment with **C1**, **C2**, **C3**, ligands **L1**, **L2**, **L3** or CDDP at concentrations corresponding to IC_{50}. Representative dot plots of three independent experiments are given, presenting intact cells at lower-left quadrant, FITC(−)/PI(−); early apoptotic cells at lower-right quadrant, FITC(+)/PI(−); late apoptotic or necrotic cells at upper-right quadrant, FITC(+)/PI(+); and necrotic cells at upper-left quadrant, FITC(−)/PI(+). (B) Apoptosis and necrosis were quantified by FACS after Annexin-V-FITC and PI labeling after 6 or 24 h treatment; bar graphs represent mean ± SD in at least three independent experiments.

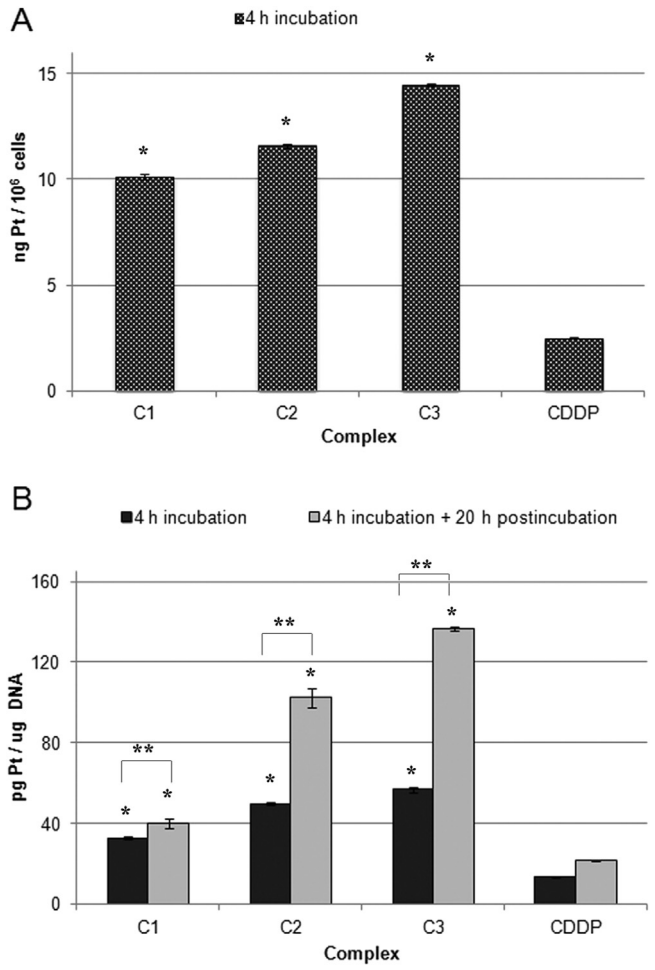

Fig. 5. Diagrams presenting quantitative determination of (A) total intracellular platinum(II) accumulation in HeLa cells after 4 h treatment; (B) Platinum(II) content in DNA, in HeLa cells, obtained by ICP-MS analysis, after 4 h treatment (with 10 mM of **C1–C3, L1–L3 or CDDP) and after 20 h post-incubation in drug-free medium**; Bar graphs represent mean ± SD of three independent experiments. $^{*}p < 0.05$ versus *cisplatin* (Kruskal Wallis test); $^{**}p < 0.01$ (Wilcoxon signed rank test with continuity correction: V = 0, *p* value 0.002).

pointed toward some other physicochemical properties, which might be involved in **C3** accumulation. Lipophilicity-independent mechanism, such as reactivity of platinum complexes and ability of formation of reactive aqua or chlorido species, were suggested by several authors, to be a factor affecting transport by proteins [64–66]. Studies by Keppler et al. [64,65], indicated that for platinum complexes with bulky diaminocyclohexane ligands, both reactivity and appropriate lipophilicity are important factors, that influence cellular accumulation and biological activity, since to high lipophilicity could hamper platinum DNA-adduct formation. Additional studies are needed in order to better understand the mechanism of enhanced intracellular accumulation of platinum complexes of structure *cis*-[$PtI_2(L^{1-3})$] (**C1**–**C3**), as well as to elucidate their potential in *cisplatin* resistant cell variants.

3.9. Results of ICP-MS measurement of platinum(II)-DNA binding

Platinum based drugs exert their cytotoxic effect by the formation of DNA cross-links. In order to investigate the actual platination of DNA induced by novel complexes of structural formula *cis*-[$PtI_2(L^{1-3})$], DNA-binding study was performed in HeLa cells. Cells were collected immediately after treatment (4 h), or the medium was discarded following treatment (4 h), and incubation continued for an additional 20 h, in platinum-free growth medium. The nuclear DNA was isolated and quantified. Platinum(II)-DNA content was measured by ICP-MS (Fig. 5B). The results showed that complexes bind to cellular DNA much more efficiently comparing to CDDP. Following short-term treatment (4 h), tested complexes already exhibited markedly higher DNA binding (pg Pt/μg DNA), which increased in order: 13.3 ± 0.2 (**CDDP**) < 32.9 ± 1.3 (**C1**) < 49.8 ± 0.6 (**C2**) < 56.9 ± 0.4 (**C3**). Statistically significant difference ($^{**}p = 0.01$; Kruskal Wallis test) in DNA binding between tested complex **C1**–**C3** and *cisplatin*, was revealed at both time points. Following 20 h post-treatment there was increase of DNA-platination (pg Pt/μg DNA), for all tested complexes, by a factor of approximately: 1.6 (for **CDDP**); 1.2 (for **C1**); 2 (for **C2**); or 2.4 (for **C3**). It should be noted that under the treatment conditions (20 h post-incubation in drug free medium), efflux of drug was allowed, but still time dependent increase of DNA-platination was significant, ($p = 0.002$; Wilcoxon signed rank test) for all tested complexes (Fig. 5B).

Data obtained are in accordance to the results of drug accumulation study, which pointed out effective intracellular accumulation of platinum-iodido compounds, (especially **C2** and **C3** with pentyl-esters groups), comparing to *cisplatin*. The cytotoxicity of tested complexes may be explained by the fact that they act as a DNA binding agents which penetrate cells efficiently and are delivered to the nucleus where they form massive adducts with DNA, and induce cell death [17,67].

3.10. Results of morphological analysis of cell death

Morphological changes in the cell shape and chromatin condensation are basic and the oldest criteria to discriminate between apoptotic and necrotic mode of cell death [68]. In order to more precisely investigate mode of cell death induced by tested agents, morphological examination of cell death was performed for 6 h and 24 h of drug action at IC_{50} concentration, by fluorescence microscopy, using acridine orange/ethidium bromide staining. Results obtained are presented as micrographs in Fig. 6A and B. Analysis of morphological characteristics of cells showed that cells started to change their shape (they shrunk and started to round up), 6 h after the continuous treatment with **C1**, **C3** as well as **L1**, **L3** (Fig. 6A). Different types of alterations were detected: (a) irregularly shaped marginal chromatin condensation; (b) condensed chromatin and nucleus inverted in one side; (c) enlarged nucleus colored red because of plasma membrane lysis. These alterations were even more expressed following 24 h treatment (Fig. 6B). Morphological changes: (a) and (b) induced prevalently by ligands **L1**, **L3** and complexes **C1**, C**3** were characteristic for apoptosis and were described in the literature [49]. **C2** as well as **L2** induced rather enlarged nucleus and orange chromatin staining, which were indicative for plasma membrane lysis. Results are compatible to the results of the apoptosis study by Annexin-V-FITC binding which showed the least potential of **C2** and **L2** for apoptosis induction and time-dependent increase of the percentage of necrotic cells. There are accumulating evidences of existence of alternative, molecularly divergent cell death processes, relative to apoptosis, that might be involved in response to cytotoxic insult [59,68,69]. Markedly higher intracellular accumulation of tested compounds, comparing to *cisplatin*, according to ICP-MS study, may cause consequently, other cellular injuries, or obstruct progression of cell death through a typical apoptotic process.

4. Conclusion

Syntheses of three novel ligands (**L1**–**L3**) and corresponding Pt(II) iodido complexes (**C1**–**C3**) were described. The compounds were characterized by elemental analysis, UV/Vis, IR, NMR

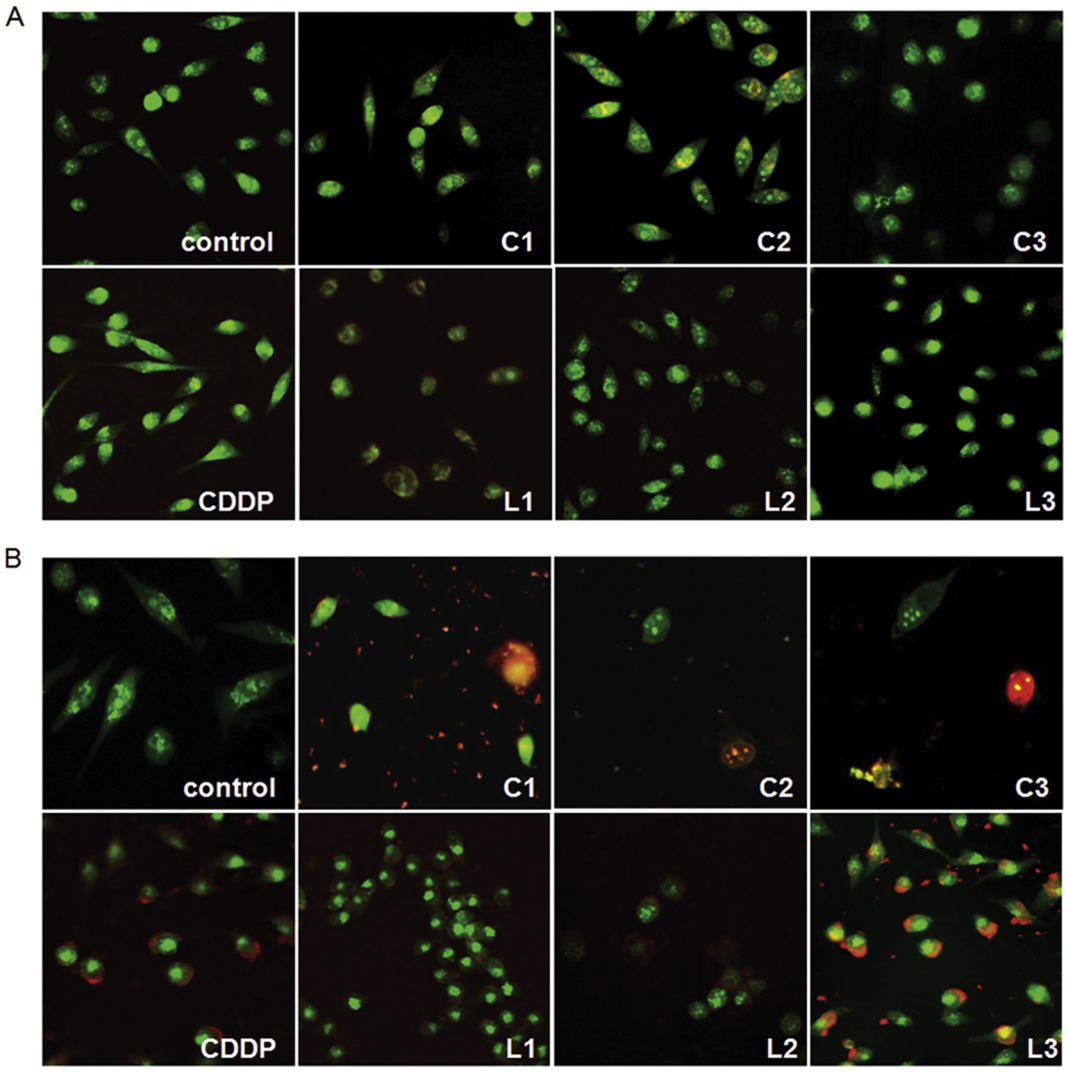

Fig. 6. Fluorescent micrographs presenting HeLa cells treated with the tested compounds or CDDP at concentrations corresponding to IC_{50} after (A) 6 h treatment or (B) 24 h treatment. Untreated cells were used as control. The fluorescent microscope Axio Observer Z1, using AxioVision imaging software (Carl Zeiss MicroImaging GmbH) was used. Acridine orange is a vital dye and will stain both live and dead cells. Ethidium bromide stains only cells that have lost membrane integrity. Untreated control cells were live cells which appeared uniformly green. Micrographs (6A) presents early apoptotic cells that started to gain round shape, detected upon short-term (6 h) treatment with **C1** and **C3** as well **L1** and **L3**. Cells were stained with green and contained bright green dots in the nuclei as a consequence of chromatin condensation and nuclear fragmentation. **C2** seemed to induce some changes characteristic for necrosis, since cells incorporated ethidium bromide (stained orange), but had a nuclear morphology resembling that of viable cells, with no condensed chromatin. Micrograph (6B) presents apoptotic, late apoptotic and necrotic cells, detected upon treatment with **C1**–**C3** at IC_{50} for 24 h. Late apoptotic cells incorporated ethidium bromide and therefore stained orange, but, in contrast to necrotic cells, the late apoptotic cells showed condensed and fragmented nuclei. Ligands **L1**–**L3** also induced apoptotic changes, similar as **CDDP**. (For interpretation of the references to colour in this figure legend, the reader is referred to the web version of this article.)

spectroscopy and mass spectrometry. All data suggest that ligands were coordinated for platinum center *via* nitrogen donor atoms.

Coordination of (**L1**–**L3**) to the platinum(II) center, resulted in increased cytotoxicity of the complexes comparing to ligands. Cytotoxic activity of novel platinum(II) iodido complexes, was comparable to *cisplatin* or markedly superior, as in LS-174 cells. *In vitro* cytotoxic and anticancer potential of alkyl esters of functionalized (*S*,*S*)-ethylenediamine-*N*,*N*′-propanoic acid and the corresponding platinum or ruthenium complexes, have been already reported [26,27]. In accordance to the previous studies, comparison of structure and activity in the present study, revealed variations of cytotoxicity of complexes **C1**–**C3** in relation to the lipophilic parameters (C log P), influenced by the alkyl ester chain in the carrier ligands. In addition, there was an increase of the intracellular accumulation and DNA platination of tested complexes in relation of length and branching of the ester chain, in sequence: **C1** (isobutyl) < **C2** (*n*-pentyl) < **C3** (isopentyl).

ICP-MS study revealed that tested complexes accumulated in the cells much more efficiently and possessed better affinity for DNA binding in comparison to *cisplatin*, in HeLa cells. Generation of considerable "sub-G1" peak, following treatment with **C1**–**C3**, suggested than DNA cleavage appeared in a course of cell death [58], but unlike to *cisplatin*, there was an absence of other substantial cell cycle alterations. According to Annexin-V-FITC assay and morphological studies, amount of apoptotic cell population did not correlate to the corresponding IC_{50} values of tested compounds. Although ligands exhibited apoptotic potential, mode of action of complexes could not be simply predicted upon structure or cytotoxicity of ligands, and only complex **C1** showed higher potential for apoptosis induction in comparison to the **L1** and *cisplatin*. Results obtained allowed us to conclude that diiodido-diamine Pt(II) complexes, exert their cytotoxic effect, as DNA binding agents, that enter cells efficiently and are delivered to the nucleus, which is in agreement to the numerous literature data considering biological

action of diamine platinum compounds [58,61–64]. However, tested complexes seem to exhibit different mode of action, comparing to *cisplatin*, characterized by both apoptotic and necrotic cell changes. It seems that the onset of necrotic processes might appear as a consequence of multiple cellular effects and injuries, particularly at the observed higher rate of intracellular accumulation.

Certainly factors that favor platinum complexes uptake into the cell nuclei and subsequent efficient DNA damage, may contribute to their overall potential in *cisplatin*-sensitive/resistant cell lines. Resistance is one of the major limitations of platinum anticancer chemotherapy and is the consequence of multifactorial events, among which, the reduced drug accumulation presents the most frequently observed phenomenon [60,62,70,71]. Structure-activity comparison of the novel platinum complexes *cis*-[$PtI_2(L^{1-3})$] (**C1**–**C3**), indicated that proper lipophilicity of the (*S*,*S*)-1,3-propanediamine-*N*,*N*′-di-2-(3-cyclohexyl)propanoic acid esters, in combination to the substitution kinetics of iodide ligands in physiological conditions, both favor markedly better intracellular accumulation and DNA binding, in comparison to *cisplatin*.

Altogether novel platinum iodide complexes showed promising *in vitro* biological properties and should be further investigated for their mechanism of action in *cisplatin* resistant variants.

Acknowledgments

This work was supported by the Ministry of Education, Science and Technological Development of the Republic of Serbia, grant numbers 172035 and III 41026, Innovative project number 451-03-2372-IP. The authors acknowledge the support of the FP7 RegPot project FCUB ERA GA No. 256716. The EC does not share responsibility for the content of the article. We are also grateful to Dr. Ivan Vučković who contributed to the interpretation of NMR spectra of the synthesized complexes in the manuscript, to Mrs. Maja Gruden-Pavlović and Stepan Stepanović for computational studies. Also, we are grateful to Mrs. Dušica Gavrilović for the assistance on statistical analysis.

Appendix A. Supplementary data

Supplementary data related to this article can be found at http://dx.doi.org/10.1016/j.ejmech.2014.05.060.

References

[1] C. Avendaño, J.C. Menédez, Medicinal Chemistry in Anticancer Drugs, first ed., Elsevier, Amsterdam, 2008.
[2] E. Alessio, Bioinorganic Medicinal Chemistry, first ed., Wiley-VCH, Weinheim, 2011.
[3] I. Romero-Canelon, P.J. Sadler, Inorg. Chem. 52 (2013) 12276–12291.
[4] C.G. Hartinger, M. Groessl, S.M. Meier, A. Casinif, P.J. Dyson, Chem. Soc. Rev. 42 (2013) 6186–6199.
[5] I. Lakomska, M. Fandzloch, T. Muziol, T. Liz, J. Jezierska, Dalt. Trans. 42 (2013) 6219–6226.
[6] A.I. Matesans, I. Leitao, P. Souza, J. Inorg. Biochem. 125 (2013) 26–31.
[7] A.G. Quiroga, J. Inorg. Biochem. 114 (2012) 106–112.
[8] H.P. Varbanov, M.A. Jakupec, A. Roller, F. Jensen, M. Galanski, B.K. Keppler, J. Med. Chem. 56 (2013) 330–344.
[9] N.J. Wheate, S. Walker, G.E. Craig, R. Oun, Dalt. Trans. 39 (2010) 8113–8127.
[10] S.H. Oberoi, V.N. Nukolova, Y. Zhao, S.M. Cohen, A.V. Kabanov, T.K. Bronich, Chemother. Res. Pract. 2012 (2012) 905796–905806.
[11] P. Karmakar, S. Ray, S. Mallick, B.K. Bera, A. Mandal, S. Mondal, A.K. Ghosh, J. Chem. Sci. 125 (2013) 1133–1143.
[12] K. Suntharalingam, O. Mendoza, A.A. Duarte, D.J. Mann, R. Vilar, Metallomics 5 (2013) 514–523.
[13] U. Jungwirth, D.N. Xanthos, J. Gojo, A.K. Bytzek, W. Koerner, P. Heffeter, S. Abramkin, M.A. Jakupec, C.G. Hartinger, U. Windberger, M. Galanski, B.K. Keppler, W. Berger, Mol. Pharmacol. 81 (2012) 719–728.
[14] I. Kostova, Recent. Pat. Anti-Cancer 1 (2006) 1–22.
[15] R.C. Todd, S.J. Lippard, Metallomics 1 (2009) 280–291.
[16] M.A. Jakupec, M. Galanski, V.B. Arion, C.G. Hartinger, B.K. Keppler, Dalt. Trans. (2008) 183–194.
[17] L. Messori, L. Cubo, C. Gabbiani, A. Álvarez-Valdés, E. Michelucci, G. Pieraccini, C. Ríos-Luci, L.G. León, J.M. Pardón, C. Navarro-Ranninger, A. Casini, A.G. Quiroga, Inorg. Chem. 51 (2012) 1717–1726.
[18] A. Casini, C. Gabbiani, E. Michelucci, G. Pieraccini, G. Moneti, P.J. Dyson, L. Messori, J. Biol. Inorg. Chem. 14 (2009) 761–770.
[19] V. Pichler, S.M. Valiahdi, M.A. Jakupec, V.B. Arion, M. Galanski, B.K. Kepler, Dalt. Trans. 40 (2011) 8187–8192.
[20] L. Messori, A. Casini, C. Gabbiani, E. Michelucci, L. Cubo, C. Ríos-Luci, J.M. Pardón, C. Navarro-Ranninger, A.G. Quiroga, ACS Med. Chem. Lett. 1 (2010) 381–385.
[21] A.R. Timerbaev, C.G. Hartinger, S.S. Aleksenko, B.K. Keppler, Chem. Rev. 106 (2006) 2224–2248.
[22] T. Parro, M.A. Medrano, L. Cubo, S. Munoz-Galvan, A. Carnero, C. Navarro-Ranninger, A.G. Quiroga, J. Inorg. Biochem. 127 (2013) 182–187.
[23] G.N. Kaludjerović, H. Schmidt, S. Schwieger, C. Wagner, R. Paschke, A. Dietrich, T. Mueller, D. Steinborn, Inorg. Chim. Acta 361 (2008) 1395–1404.
[24] G.N. Kaludjerović, D. Miljković, M. Momčilović, V.M. Djinović, M. Mostarica Stojković, T.J. Sabo, V. Trajković, Int. J. Cancer 116 (2005) 479–486.
[25] G.N. Kaludjerović, V.M. Djinović, Z. Juranić, T. Stanojković, T.J. Sabo, J. Coord. Chem. 59 (2006) 815–819.
[26] J.M. Lazić, Lj. Vučićević, S. Grgurić-Šipka, K. Janjetović, G.N. Kaludjerović, M. Misirkić, M. Gruden-Pavlović, D. Popadić, R. Paschke, V. Trajković, T.J. Sabo, ChemMedChem 5 (2010) 881–889.
[27] S. Misirlic Dencic, J. Poljarevic, U. Vilimanovich, A. Bogdanovic, A.J. Isakovic, T. Kravic Stevovic, M. Dulovic, N. Zogovic, A.M. Isakovic, S. Grguric-Sipka, V. Bumbasirevic, T. Sabo, V. Trajkovic, I. Markovic, Chem. Res. Toxicol. 25 (2012) 931–939.
[28] A. Savić, S. Misirlic-Dencic, Marija Dulovic, Lj.E. Mihajlović, M. Jovanovic, S. Grgurić-Šipka, I. Markovic, T.J. Sabo, Bioorg. Chem. 54 (2014) 73–80.
[29] R.N. Keller, T. Moeller, Inorg. Synth. 7 (1963) 247–250.
[30] http://www.vcclab.org/ (accessed March 2011).
[31] I.V. Tetko, V.Y. Tanchuk, J. Chem. Inf. Comp. Sci. 42 (2002) 1136–1145.
[32] I.V. Tetko, V.Y. Tanchuk, A.E. Villa, J. Chem. Inf. Comp. Sci. 41 (2001) 1407–1421.
[33] http://www.cambridgesoft.com (accessed March 2011).
[34] (a) E.J. Baerends, T. Ziegler, J. Autschbach, D. Bashford, A. Bérces, F.M. Bickelhaupt, C. Bo, P.M. Boerrigter, L. Cavallo, D.P. Chong, L. Deng, R.M. Dickson, D.E. Ellis, M. van Faassen, L. Fan, T.H. Fischer, C. Fonseca Guerra, M. Franchini, A. Ghysels, A. Giammona, S.J.A. van Gisbergen, A.W. Götz, J.A. Groeneveld, O.V. Gritsenko, M. Grüning, S. Gusarov, F.E. Harris, P. van den Hoek, C.R. Jacob, H. Jacobsen, L. Jensen, J.W. Kaminski, G. van Kessel, F. Kootstra, A. Kovalenko, M.V. Krykunov, E. van Lenthe, D.A. McCormack, A. Michalak, M. Mitoraj, S.M. Morton, J. Neugebauer, V.P. Nicu, L. Noodleman, V.P. Osinga, S. Patchkovskii, M. Pavanello, P.H.T. Philipsen, D. Post, C.C. Pye, W. Ravenek, J.I. Rodríguez, P. Ros, P.R.T. Schipper, G. Schreckenbach, J.S. Seldenthuis, M. Seth, J.G. Snijders, M. Solà, M. Swart, D. Swerhone, G. te Velde, P. Vernooijs, L. Versluis, L. Visscher, O. Visser, F. Wang, T.A. Wesolowski, E.M. van Wezenbeek, G. Wiesenekker, S.K. Wolff, T.K. Woo, A.L. Yakovlev, ADF2013, SCM, Theoretical Chemistry, Vrije Universiteit, Amsterdam, The Netherlands, http://www.scm.com. (b) C.F. Guerra, J.G. Snijders, G. teVelde, E. Baerends, Theor. Chem. Acc. 99 (1998) 391–403;
(c) G. te Velde, F.M. Bickelhaupt, E.J. Baerends, C. Fonseca Guerra, S.J.A. van Gisbergen, J.G. Snijders, T. Ziegler, J. Comput. Chem. 22 (2001) 931–967.
[35] N.C. Handy, A. Cohen, Molec. Phys. 99 (2001) 403–412.
[36] J.P. Perdew, K. Burke, M. Ernzerhof, Phys. Rev. Lett. 77 (1996) 3865–3868.
[37] M. Swart, A.W. Ehlers, K. Lammertsma, Molec. Phys. 102 (2004) 2467–2474.
[38] E. van Lenthe, E.J. Baerends, J. Comput. Chem. 24 (2003) 1142–1156.
[39] E. van Lenthe, A. Ehlers, E.J. Baerends, J. Chem. Phys. 110 (1999) 8943–8953.
[40] (a) A. Bérces, R.M. Dickson, L. Fan, H. Jacobsen, D. Swerhone, T. Ziegler, Comput. Phys. Commun. 100 (1997) 247–262;
(b) H. Jacobsen, A. Bérces, D. Swerhone, T. Ziegler, Comput. Phys. Commun. 100 (1997) 263–276.
[41] (a) A. Klamt, G. Schüürmann, J. Chem. Soc. Perkin Trans. 2 (1993) 799–805;
(b) A. Klamt, J. Phys. Chem. 99 (1995) 2224–2235;
(c) A. Klamt, V. Jones, J. Chem. Phys. 105 (1996) 9972–9981.
[42] (a) C.C. Pye, T. Ziegler, Theor. Chem. Acc. 101 (1999) 396–408;
(b) M. Swart, E. Rösler, F.M. Bickelhaupt, Eur. J. Inorg. Chem. (2007) 3646–3654.
[43] R. Supino, Methods in molecular biology, in: S. O'Hare, C.K. Atterwill (Eds.), Vitro Toxicity Testing Protocols, Humana Press, New Jersey, 1995, pp. 137–149.
[44] M.G. Ormerod, Analysis of DNA-general methods, in: M.G. Ormerod (Ed.), Flow Cytometry, a Practical Approach, Oxford University Press, New York, 1994, pp. 119–125.
[45] N.K. Banda, W.C. Satterfield, A. Dunlap, K.S. Steimer, R. Kurrle, T.H. Finkel, Apoptosis 1 (1996) 49–62.
[46] P. Heitland, H.D. Köster, Clin. Chim. Acta 356 (2006) 310–318.
[47] A. Savic, M. Dulovic, J.M. Poljarevic, S. Misirlic Dencic, M. Jovanovic, A. Bogdanovic, V. Trajkovic, T.J. Sabo, S. Grguric-Sipka, I. Markovic, ChemMedChem 6 (2011) 1884–1891.
[48] J.M. Vujic, M. Cvijovic, G.N. Kaluderovic, M. Milovanovic, B.B. Zmejkovski, V. Volarevic, N. Arsenijevic, T.J. Sabo, S.R. Trifunovic, Eur. J. Med. Chem. 45 (2010) 3601–3606.

[49] S. Arandjelovic, Z. Tesic, Z. Juranic, S. Radulovic, M. Vrvic, B. Potkonjak, Z. Ilic, J. Exp. Clin. Cancer Res. 21 (2002) 519–526.
[50] M.J. Cleare, P.C. Hydes, B.W. Malerbi, D.M. Watkins, Biochimie 60 (1978) 835–850.
[51] J. Zhao, S. Gou, F. Liu, Y. Sun, C. Gao, Inorg. Chem. 52 (2013) 8163–8170.
[52] S. Moradell, J. Lorenzo, A. Rovira, M.S. Robillard, F.X. Avilés, V. Moreno, R. de Llorens, M.A. Martinez, J. Reedijk, A. Llobet, Inorg. Biochem. 96 (2003) 493–502.
[53] V. Alverdi, L. Giovagnini, C. Marzano, R. Seraglia, F. Bettio, S. Sitran, R. Graziania, D. Fregona, J. Inorg. Biochem. 98 (2004) 1117–1128.
[54] E. Budzisz, M. Miernicka, I.P. Lorenz, P. Mayer, U. Krajewska, M. Rozalski, Polyhedron 28 (2009) 637–645.
[55] D. Wang, S.J. Lippard, Nat. Rev. Drug. Discov. 4 (2005) 307–320.
[56] M.S. Benassi, A. Chiechi, F. Ponticelli, L. Pazzaglia, G. Gamberi, L. Zanella, M.C. Manara, P. Perego, S. Ferrari, P. Picci, Cancer Lett. 250 (2007) 194–205.
[57] X. Huang, H.D. Halicka, F. Traganos, T. Tanaka, A. Kurose, Z. Darzynkiewicz, Cell. Prolif. 38 (2005) 223–243.
[58] E.H. Vock, W.K. Lutz, P. Hormes, H.D. Hoffmann, S. Vamvakasa, Mutat. Res. 413 (1998) 83–94.
[59] S.M. Sancho-Martínez, F.J. Piedrafita, J.B. Cannata-Andía, J.M. López-Novoa, F.J. López-Hernández, Toxicol. Sci. 122 (2011) 73–85.
[60] Z. Darzynkiewicz, H. Zhao, H.D. Halicka, P. Rybak, J. Dobrucki, D. Wlodkowic, Crit. Rev. Clin. Lab. Sci. 49 (2012) 199–217.
[61] F. Zunino, P. Perego, S. Pilotti, G. Pratesi, R. Supino, F. Acramone, Pharmacol. Ther. 76 (1997) 177–185.
[62] C. Lanzi, P. Perego, R. Supino, S. Romanelli, T. Pensa, N. Carenini, I. Viano, D. Colangelo, R. Leone, P. Apostoli, G. Cassinelli, R.A. Gambetta, F. Zunino, Biochem. Pharmacol. 55 (1998) 1247–1254.
[63] M. Alesio, I. Zanellato, I. Bonarrigo, E. Gabano, M. Ravera, D. Osella, J. Inorg. Biochem. 129 (2013) 52–57.
[64] I. Buβ, G.V. Kalayda, A. Lindauer, M.R. Reithofer, M. Galanski, B.K. Keppler, U.J. Jaehde, J. Biol. Inorg. Chem. 17 (2012) 699–708.
[65] I. Buβ, D. Garmann, M. Galanski, G. Weber, G.V. Kalayda, B.K. Keppler, U. Jaehde, J. Inorg. Biochem. 105 (2011) 709–717.
[66] A. Ghezzi, M. Aceto, C. Cassino, E. Gabano, D. Osella, J. Inorg. Biochem. 98 (2004) 73–78.
[67] V.R. Menon, E.J. Peterson, K. Valerie, N.P. Farrell, L.F. Povirk, Biochem. Pharmacol. 86 (2013) 1708–1720.
[68] J.X. Xiao, G.Q. Huang, C.P. Zhu, D.D. Ren, S.H. Zhang, Toxicol. In Vitro 21 (2007) 820–826.
[69] S.M. Sancho-Martínez, L. Prieto-García, M. Prieto, J.M. López-Novoa, F.J. López-Hernández, Pharmacol. Ther. 136 (2012) 35–55.
[70] P. Marqués-Gallego, G.V. Kalayda, U. Jaehde, H.D. Dulk, J. Brouwer, J. Reedijk, J. Inorg. Biochem. 103 (2009) 791–796.
[71] L. Martelli, F. Di Mario, P. Botti, E. Ragazzi, M. Martelli, L. Kelland, Biochem. Pharmacol. 74 (2007) 20–27.